6.5   A CLIMATOLOGICAL AND COMPOSITE STUDY OF COLD SEASON BANDED PRECIPITATION IN THE NORTHEAST UNITED STATES

*David R. Novak, Lance F. Bosart, Daniel Keyser
University at Albany, State University of New York, Albany, New York

Jeff S. Waldstreicher
*National Weather Service Eastern Region, Scientific Services Division,
Bohemia, New York*

1. INTRODUCTION

Mesoscale band formation in extratropical cyclones has been a popular focus for study in improving Quantitative Precipitation Forecasts (QPF) since these features can dramatically affect the intensity, timing, and subsequent accumulation of precipitation. Several case studies in the northeast United States (US) have established the occurrence of significant mesoscale banding associated with frontogenesis and small moist symmetric stability (e.g., Sanders and Bosart 1985; Nicosia and Grumm 1999), but a comprehensive investigation establishing the frequency, variety, dynamical forcing, and environmental stability of significant mesoscale banding has not been conducted. In the past, a lack of observational data on the scale of banded structures prohibited such a comprehensive investigation; however, the operational deployment of the WSR–88D national radar network and the recent availability of gridded daily precipitation datasets allows examination of precipitation systems in their entirety, and provides a standardized database to identify mesoscale bands.

This study utilizes these recent developments to conduct a climatological and composite study of mesoscale band formation in the northeast US. A subjective band classification scheme based on observed radar signatures was first developed in order to document mesoscale banding in the northeast US. This scheme was applied to five recent cold seasons to provide a climatology of banded precipitation events during the cold season. The resultant dataset of banded events was used for composite investigations to document how the synoptic flow influences cyclone substructure. Furthermore, the composites document the environments of the different types of bands through assessments of frontogenetical forcing, stability, and moisture.

2. METHODOLOGY

The area of study is shown in Fig. 1. Although a portion of southeast Canada is included in the domain, the study was restricted to data from the US radar network. The Unified Precipitation Dataset

---

Corresponding author address: David Novak, Dept. of Earth and Atmospheric Sciences, University at Albany, SUNY, 1400 Washington Ave., Albany, NY 12222 email: dnovak@atmos.albany.edu

(UPD) (http://www.cdc.noaa.gov/cdc/data.unified.html) and the Daily Weather Maps series were utilized to identify cases for study during the cold season (October through April) in April 1995 and from October 1996 (when the radar network was fully established) through April 2001. Only systems exhibiting precipitation greater than 25 mm, or 12.5 mm liquid equivalent in the case of frozen precipitation, during a 24 h period at a location within the study area were selected as cases for study. Out of the 111 cases identified for study, 88 had available composite radar data.

Fig. 1. Topographical map of study area.

A subjective band classification scheme (Table 1) was devised by examining the composite radar data, consulting with operational forecasters, and referencing previous literature (e.g., Houze et al. 1976). Three dominant band categories are proposed (single, multiband, and narrow cold-frontal) with the transitory structure serving as a bridge between the significantly banded structures and nonbanded cases. This classification scheme was then applied to the above 88 cases for which composite radar data were available, providing a limited climatology of banded structures in the northeast US.

In order to develop composite stratifications, a cyclone-relative composite of the single-band distribution was developed. Surface cyclone positions at the analysis time most representative of the banded structure were determined by utilizing the National Centers for Environmental Prediction (NCEP)/ National Centers for Atmospheric Research (NCAR) reanalysis dataset (Kalnay et al. 1996), and the band location at this time was determined from radar.

Cyclone-relative composites were calculated to identify flow regimes conducive to the development of single-banded structures. The smoothed and interpolated 80 km grids from the operational Eta model initial

analyses and 6 h forecasts were utilized for this purpose. FORTRAN code was developed to center the gridded data at the surface cyclone position, and then to average basic diagnostic fields of all events included in the composite at 17 levels (every 50 hPa from 1000 to 200 hPa). Derived fields were calculated using GEMPAK software.

3. RESULTS

3.1 Climatology

The results of the application of the band classification scheme to the 88 study cases is shown in Table 2. The occurrence of a banded structure within a case was termed an "event." Despite the rigorous criteria, 162 banded events were noted during the period, demonstrating the frequency with which mesoscale banding challenges forecasters. Single-banded structures were the most common, followed by transitory, narrow cold-frontal, and multibanded structures. It is important to note that cases frequently exhibited more than one banded event and occasionally more than one type of banded structure, during the case evolution. In fact, some cases exhibited interaction between multi and single-banded structures with the multibands merging into a dominant single band. The 13 nonbanded cases are of particular interest since they will help elicit the difference between banded and nonbanded cases.

Composite study focused on the single-banded structure, since it was the most common in the region. A cyclone-relative distribution of the single-banded events is shown in Fig. 2. Over 70% of the single bands exhibit some portion of their length in the northwest quadrant relative to the surface cyclone, occurring in the comma-head portion of the cyclone, while the remaining single bands were found ahead of the cyclone.

3.2 Composites

The next task was to develop cyclone-relative composites for banded and nonbanded events. Composite stratifications were proposed according to band location relative to the surface cyclone. Figure 3 summarizes the composite results of all analysis times exhibiting bands in the northwest quadrant relative to the surface cyclone, with geography provided for reference. A robust cyclone is present off the Virginia coast (Fig. 3a) associated with a negatively tilted 500 hPa trough (Fig. 3c). A strong jet is rounding the base of the trough, and a weaker jet is found in the confluence region over southeast Canada (Fig. 3d). This pattern resembles the jet configuration Kocin and Uccellini (1990, 58–62) cited for northeast US. snowstorms. A large-scale deformation zone associated with frontogenesis is present northwest of the surface cyclone (Fig. 3b). This location is coincident with the mean band position across central Pennsylvania (not shown). This coincidence is of particular interest since several studies (e.g., Emanuel 1985; Sanders and Bosart 1985; Nicosia and Grumm 1999) have demonstrated that frontogenesis in the presence of weak symmetric stability supports mesoscale banding.

The nonbanded composite exhibits a much weaker cyclone (Fig. 4a), found in the confluent entrance region of the Atlantic jet (Fig. 4d). Significant precipitation was associated with cases included in this composite, but the absence of a closed midlevel circulation (Figs. 4b–d) precluded deformation and frontogenesis northwest of the surface cyclone, limiting band development. Although midlevel confluence ahead of the surface cyclone contributes to frontogenesis (Fig. 4c), it is weaker in the lower levels (shown in cross-section analysis) than in the northwest banded composite.
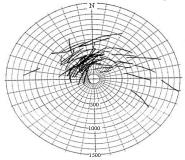

Fig. 2. Distribution of single bands relative to surface cyclone position (origin). Each black line represents the axis of a single band at the most representative analysis time. Radial distance scale is in kilometers.

3.3 Composite cross sections

Cross sections were taken through the respective composite frontogenesis maxima to investigate the environmental stability and frontogenetical forcing of each composite. Figure 5 summarizes the respective environments. Frontogenetical forcing is readily evident in both cross sections (Figs. 5a,c), with a sloping frontogenesis maximum found within each frontal zone. A sloping updraft is found on the equatorward flank of each frontal zone (Figs. 5b,d), consistent with a thermally direct circulation induced by frontogenesis; however, the northwest composite cross section exhibits a stronger, narrower, and deeper updraft than the nonbanded composite cross section. This difference may be explained by noting that the northwest composite frontal zone exhibits a more upright configuration than the nonbanded composite frontal zone, consistent with smaller static stability. As shown by Emanuel (1985), the frontogenetical response in the presence of weak symmetric stability takes the form of a concentrated updraft on the equatorward flank of the frontal zone. It appears that the northwest composite cross section exhibits this signature. Conversely, the nonbanded composite cross section exhibits a weaker and broader vertical response, consistent with larger static stability. Also, the nonbanded composite is much drier than the northwest composite (compare Figs. 5b and 5d).

4. SUMMARY

A climatology of banded precipitation events in the northeast US during the cold season revealed the

frequency with which significant mesoscale banding events affect the region. Further investigation of the single-banded events highlighted banded structure in the comma-head portion of storms.

A comparison of the northwest banded and nonbanded composite fields revealed that the formation of a closed midlevel circulation resulted in the development of a confluent asymptote northwest of the surface cyclone, leading to frontogenesis and subsequent band development. The absence of a closed midlevel circulation in the nonbanded composite precluded the development of a confluent asymptote and subsequent frontogenesis northwest of the surface cyclone. Furthermore, the upright nature of the northwest composite frontal zone supported banded structure. Similar results have been reproduced by Novak and Horwood (2002) in a case study of banded structure. These results suggest that assessment of the forecast amplitude and depth of a disturbance in conjunction with cross-section analysis of the forecast frontal structure can be used to discriminate between potential banded and nonbanded cases.

5. ACKNOWLEDGMENTS

6. REFERENCES

Emanuel, K. A., 1985: Frontal circulations in the presence of small moist symmetric stability. *J. Atmos. Sci.* **42**, 1062–1071.

Houze, R. A. Jr., P. V. Hobbs, K. R. Biswas, and W. M. Davis, 1976: Mesocale rainbands in extratropical cyclones. *Mon. Wea. Rev.*, **104**, 868–879.

Kalnay, E., and Coauthors, 1996: The NCEP/NCAR 40-Year Reanalysis Project. *Bull. Amer. Meteor. Soc.*, **77**, 437-471.

Kocin, P. J., and L. W. Uccellini, 1990: Snowstorms along the northeastern coast of the United States: 1955–1985. Amer. Meteor. Soc., 280 pp.

Nicosia, D. J., and R. H. Grumm, 1999: Mesoscale band formation in three major northeastern United States snowstorms. *Wea. Forecasting*, **14**, 346–368.

Novak, D. R., and R. S. W. Horwood, 2002: Analysis of mesoscale banded features in the 5–6 February 2001 New England snowstorm. *Preprints 19th Conference on Weather Analysis and Forecasting,* San Antonio TX.

Sanders, F., and L. F. Bosart, 1985: Mesoscale structure in the megalopolitan snowstorm of 11–12 February 1983. Part I: Frontogenetical forcing and symmetric instability. *J. Atmos. Sci.*, **42**, 1050–1061.
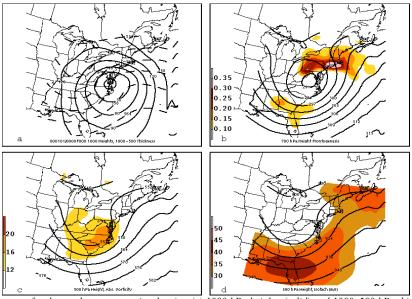
Fig. 3. Synoptic summary for the northwest composite showing (a) 1000 hPa heights (solid) and 1000–500 hPa thickness (dashed), (b) 700 hPa heights (solid) and 2-D Miller frontogenesis [shaded according to scale in ˚C (100 km)$^{-1}$ (3 h)$^{-1}$], (c) 500 hPa heights (solid) and absolute vorticity (shaded according to scale in 10^{-5} s^{-1}), and (d) 300 hPa heights (solid) and wind speed (shaded according to scale in m s^{-1}).

Table 1: Band Classification Scheme

Band Type	Band Description
Single	Linear structure > 250 km in length, ~20–100 km in width, with an intensity > 30 dBZ maintained > 2 h
Multibanded	> 3 bands with periodic spacing and of the same spatial orientation, with intensities > 10 dBZ over the background reflectivity, maintained for > 2 h
Narrow cold-frontal	Narrow (10–50 km), long (> 300 km) band found along surface cold front or in the warm sector with an intensity > 40 dBZ, maintained for > 2 h
Transitory	Structure that meets all respective criteria in a given category, except one (usually the lifetime)
Undefined	Ambiguous due to bright banding or incomplete radar data

Nonbanded	None of the above criteria are met				

Table 2: Band climatology

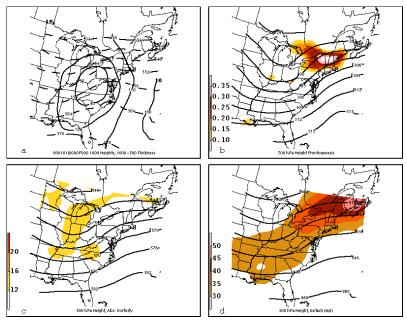| Band Type	Single	Transitory	Narrow Cold-frontal	Multi	Undefined	**Total**
Events	48	40	36	29	9	**162**

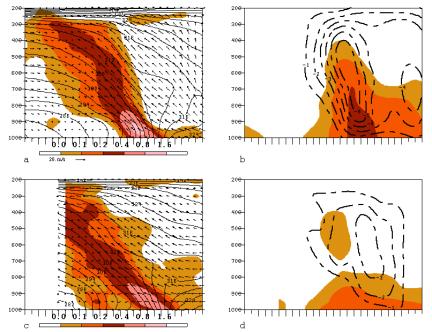*Fig. 4. As in Fig. 3, except for nonbanded composite.*

Fig. 5. Cross-section comparison through the frontogenesis maximum of the northwest composite (a, b) and nonbanded composite (c, d) (cross section orientations shown in Figs. 3b and 4b, respectively): (a) 2-D Miller frontogenesis [positive areas shaded according to scale in ˚C (100 km)$^{-1}$ (3 h)$^{-1}$], equivalent potential temperature (contoured every 3 K), and tangential full wind and vertical motion (black arrows, reference vector for horizontal wind shown near scale). (b) Relative humidity greater than 70% shaded every 10%, and vertical motion (dashed line), contoured where negative every 1 x 10^{-3} hPa s^{-1}. (c) As in Fig. 5a, except for nonbanded cross section. (d) As in Fig. 5b, except for nonbanded cross section.